Modeling urban development and its exposure to river flood risk in Southeast Asia

Tierolf, Lars; de Moel, Hans; van Vliet, Jasper

published in
Computers, Environment and Urban Systems
2021

DOI (link to publisher)
10.1016/j.compenvurbsys.2021.101620

document version
Publisher's PDF, also known as Version of record

Computers, Environment and Urban Systems 87 (2021) 101620

Contents lists available at ScienceDirect

Computers, Environment and Urban Systems

journal homepage: www.elsevier.com/locate/ceus

Modeling urban development and its exposure to river flood risk in Southeast Asia

Lars Tierolf [a,1,*], Hans de Moel [b], Jasper van Vliet [b]

[a] Earth Sciences, University of Amsterdam, 1090 GE Amsterdam, the Netherlands
[b] Institute for Environmental Studies (IVM), Vrije Universiteit Amsterdam, 1081 HV Amsterdam, the Netherlands

ARTICLE INFO

Keywords:
Flood risk analysis
Land use change
Land use model
Adaptation
Urban development

ABSTRACT

Countries in Southeast Asia have been developing quickly from a predominantly rural to predominantly urban society, leading to a rapid increase in urban land. This increase in urban land has mainly occurred in river deltas and floodplains, exposing humans and human assets to flood hazard. Here we present an assessment of current and future flood risk in five countries of mainland Southeast Asia, using a new modeling approach that accounts for differences in urban land systems. To that effect we mapped urban land on a rural-urban gradient and projected urban development until the year 2040 in two contrasting scenarios. The urban expansion scenario mainly projects the development of new urban areas, while the intensification emphasizes an increase in the number of inhabitants in already existing urban areas. Subsequently, we assessed the expected annual damage due to flood risk, using country specific exposure values for different land-system classes along the rural-urban gradient, based on typical construction materials. Results indicate that expected annual flood damage will increase in all countries and in both scenarios, ranging from +8% in Thailand to +211% in Laos. We showed that preferable development pathways are context dependent. In Cambodia and Laos, the increase in flood risk was largest for the intensification scenario, while for Myanmar, Thailand and Vietnam, the increase in flood risk was largest in the urban expansion scenario.

1. Introduction

Flooding is one of the most disruptive and frequent of natural hazards, resulting in damage to the built environment, temporal displacement and loss of life and livelihood. Between 1980 and 2018 flooding resulted in 223,482 recorded fatalities and over 1 trillion USD in damages worldwide (Munich, 2020) By the end of this century absolute flood damages may increase with a factor 20 compared to 2013 (Winsemius et al., 2016). The worldwide impact of river flooding is expected to increase, mainly due to climate change, increasing population density, and economic development in flood prone areas (Jongman, Ward, & Aerts, 2012; Vinke et al., 2017). This trend is especially relevant in mainland Southeast Asia, where the impact of economic development on future flood risk far surpasses that of climate change (Winsemius et al., 2016).

Cambodia, Laos, Myanmar, Thailand, and Vietnam together currently have a population of 246 million people, many of whom live in the floodplains and deltas of the major river systems that flow through the these countries, including the Irrawaddy, the Chao Phraya, the Red River, and the Mekong River (United Nations, 2019b). These rivers often inundate significant amounts of urban land, resulting in both economic and social damages (Varis, Kummu, & Salmivaara, 2012). Most notably, the 2011 flooding of the Chao Phraya river resulted in an estimated damage to housing of approximately 2.7 billion US dollar (The World Bank, 2011). Large differences exist between these countries in terms of economic development and governmental structures (The World Bank, 2020), but all are expected to continue developing (Webster, Cai, & Muller, 2014). The combination of economic development and urban development likely leads to a large increase in building assets exposed to flood risk (Winsemius et al., 2016).

Current practice in large scale flood risk assessments is to estimate flood risk as a product of hazard, exposure, and vulnerability (de Moel et al., 2015; Englhardt et al., 2019; Huizinga et al., 2017; (Winsemius et al., 2013)). Socio-economic development, representing the assets at risk, is expressed in the exposure and can be mapped using either a land use or a population-based approach (Jongman et al., 2012). Englhardt et al. (2019) further enhanced the representation of vulnerability by the

* Corresponding author.
E-mail addresses: lars.tierolf@vu.nl (L. Tierolf), hans.de.moel@vu.nl (H. de Moel), jasper.van.vliet@vu.nl (J. van Vliet).
[1] Current affiliation: Institute for Environmental Studies (IVM), Vrije Universiteit Amsterdam, 1081 HV Amsterdam, the Netherlands

https://doi.org/10.1016/j.compenvurbsys.2021.101620
Received 21 August 2020; Received in revised form 4 January 2021; Accepted 17 February 2021
Available online 3 March 2021

development of depth-damage curves for four building damage classes. While methods for calculating exposure values based on construction material exist (Huizinga et al., 2017), urban areas are often represented in a single land-use class in flood risk assessments. This generalization limits flood risk assessment, as differences in built environment greatly affect potential flood damage (Ward et al., 2013). Furthermore, acknowledging the variety found in human settlement allows us to project different urban futures.

Landscapes of built environments range from villages and extensive suburban neighborhoods to dense metropolitan cores (Li, van Vliet, Ke, & Verburg, 2019). These landscapes differ not only in the share of the landscape that is covered by built-up land, but also by their intensity, such as reflected in population density and building volume (van Vliet, Verburg, Grădinaru, & Hersperger, 2019). Representation of built-up land in a single urban land-use class does not do justice to the functional and morphological diversity of human settlements (Wandl, Nadin, Zonneveld, & Rooij, 2014). Different types of settlement emerge as a result of different urban development pathways. Urban sprawl results in an extensive suburban landscape characterized by a low population density and limited functional diversity (Ewing, Pendall, & Chen, 2002), while compact city development gives rise to densely developed urban areas with multistory apartment buildings through infill development (Storch, Eckert, & Pfaffenbichler, 2008). The impact of both development pathways on river flood risk is unknown, as we do not know

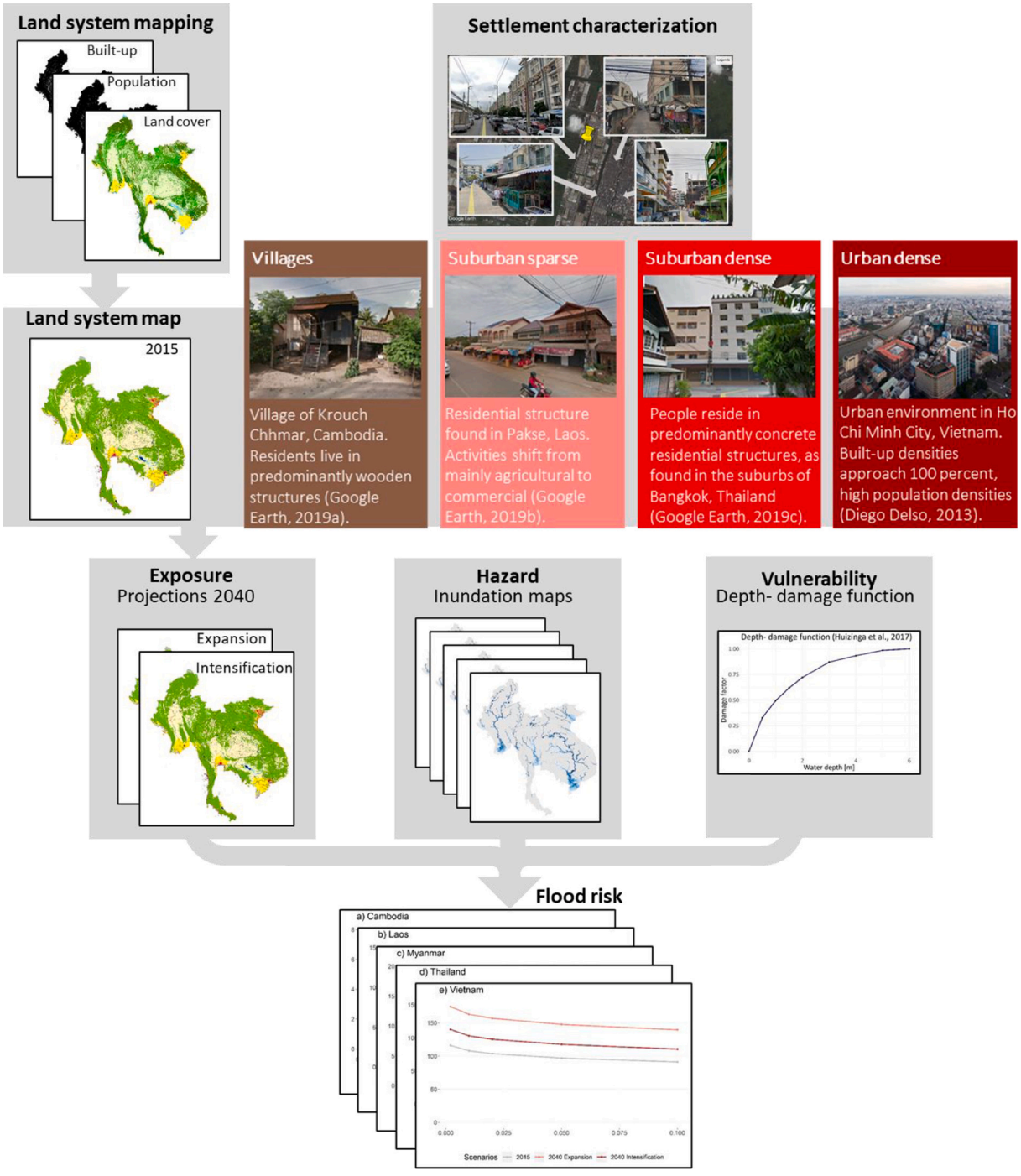

Fig. 1. Overview of the methodological approach employed in this study. The images shown in this figure were derived from (Delso, 2013; Google Earth, 2020a; Google Earth, 2020b; Google Earth, 2020c)

whether urban expansion or intensification occurs out of harm's way or further increases exposed asset value.

The aim of this paper is to assess the impact of different pathways for urban development on future risks for river flooding. Specifically, we ask whether expected annual damage is higher under an urban expansion strategy or an urban intensification strategy in each of five selected countries in Southeast Asia. To that effect we mapped urban land use on a rural-urban gradient and use this map as a starting point for model-based land-use change projections until the year 2040. Mapping built-up land on a gradient from sparsely developed rural areas to densely developed metropolitan cores is a widely applied practice in landscape science and ecology, as it allows for differentiation of varying intensities of urban land uses (Hahs & McDonnell, 2006; Kroll, Müller, Haase, & Fohrer, 2012; McDonnell & Pickett, 1990). The CLUMondo land-use model employed here differs from most existing land-use models in that it is able to simulate both urban expansion and urban intensification (Wang, van Vliet, Pu, & Verburg, 2019). Subsequently, these projections are used to assess the annual expected damage due to river flooding for both scenarios. Based on these results we discuss to what extent different urban development trajectories can contribute to sustainable land-use development.

2. Methodology

The approach for assessing future flood risk visualized in Fig. 1 broadly consists of three components. First, we characterized settlement systems based on their position on a rural-urban gradient. Settlement systems are here defined as systems of predominantly residential land use mixed with commercial and agricultural land uses. For this, we used spatial information on built-up area, population density, and land cover to identify settlement-, natural-, and agricultural land systems. Second, we use the CLUMondo model to project settlement change until the year 2040. The CLUMondo land-use model allocates land-use change based on a non-spatial demand module and an spatially explicit allocation module (van Asselen & Verburg, 2013). We configure the demand module to represent population growth, and allocate the combination of settlement systems to match this demand in each time step (one year). Since we do not model backward development or settlement abandonment, we choose to select an endpoint where there is still an increasing demand for residential area in all countries of the study area. In the third component we estimated future flood damage based on the typical building stock composition of settlement systems inferred from Google Earth imagery. We applied a single depth-damage function with inundation maps for a range of return periods and estimated the area under the risk curves to determine expected annual flood damages.

2.1. Mapping settlement systems

We mapped settlement systems along a rural-urban gradient to allow for modeling the process of gradual urban intensification. Settlement systems were mapped at a spatial resolution of 1000 m for the year 2015. Where most studies of urban development only model a single urban class, we identified four settlement system types using data from the gridded population data and built-up area map retrieved from the Global Human Settlement Layer (GHSL) (Corbane, Florczyk, Pesaresi, Politis, & Syrris, 2018; Schiavina, Freire, & MacManus, 2019). The GHSL is a free and open data product that combines satellite imagery with census data to generate population density maps. We applied different population density thresholds and subsequently assessed the classification results using Google Earth imagery until the resulting settlement system map matched the description of settlements shown in Fig. 1. In this procedure, we assessed mapped settlement cells located in densely populated metropolitan regions as well as smaller provincial cities and rural settlements. The resulting thresholds applied in the decision tree of mapping settlement systems are as follows: all pixels with >5% built-up land and > 100 persons per km^2 were considered as a settlement system. Of these pixels, all pixels with a population density > 8000 persons per km^2 were identified as *Urban dense*, all pixels with a population density > 4000 and < 7999 were classified as *Suburban dense*, all pixels with a population density > 1200 and < 3999 were classified as *Suburban sparse*, and all pixels with population density > 100 and < 1199 where classified as either Villages (<50% built-up land) or Industry/commercial land (>50% built-up).

Villages are the first settlement systems encountered on the rural-urban gradient. The built environment is associated with a low population- and building density. Inhabitants participate mostly in agricultural activities. Villages may develop into sparse suburbs as a result of an urban intensification process. Suburban sparse settlement systems are characterized by a heterogeneous building stock of wooden, concrete, and masonry structures. Further development of this settlement systems results in the emergence of dense suburban areas. The last increment on the rural-urban gradient is towards urban dense systems. The built environment here consists mainly of multi-story concrete apartment buildings with commercial spaces located on the ground floor.

Natural and agricultural land systems were mapped based on a land cover map of the study region provided by SERVIR (Patterson et al., 2018). Land cover was reclassified into categories presented in Table S2 and aggregated in 1000-m cells. Since this study focused on settlement change only, all forested land cover was combined in a single class. Land cover indicating land systems that remain static or for which land system dynamics were assumed to have a negligible effect on future flood damage were reclassified as *other*. Since built-up land cover in the GHSL slightly differs from the SERVIR land cover map, areas that were determined built-up by SERVIR and were blank in the GHSL were reclassified as *barren*. A comparison of both datasets shows that this applies to 0.09% of the total number of pixels in the compiled land system map, most of which were located in rural areas. We therefor assume that the discrepancies between land cover maps do not meaningfully affect our model results. An overview of the datasets used in this procedure is presented in Table S1.

2.2. Modeling settlement change trajectories

Two possible development pathways were hypothesized, one mainly based on urban expansion and one focusing on urban intensification. The expansion scenario gives rise to an extensive suburban landscape, characterized by single-story residential structures with a relatively low building and population density. Conversely, intensification mainly results in further densification of existing settlements, for example through infill and the construction of multistory apartment buildings. Both scenarios result in a mix of settlement expansion and intensification, with each development process being dominant in the respective scenario.

We used the CLUMondo model to create two land system projections until 2040 characterized by expansion and intensification of settlements, respectively. CLUMondo allocates land systems based on a demand for the goods and services they provide, geographic characteristics determining the local suitability for urban development, and a set of conversion rules (van Asselen & Verburg, 2013). The model is designed to simulate both land cover conversion and changes in land use intensity, as multiple land systems can provide the same service and commodities in different amounts. Through an iterative procedure the model allocates different land systems for each time step (one year), as they compete to optimize the allocation likelihood while meeting the yearly demand for land use products.

Local suitability for settlement systems was determined with a logistic regression model of multiple socio-economic and biophysical explanatory variables (Table S3). Regression models were made only for settlement system suitability, since natural and agricultural land systems were assumed to remain unchanged unless they change into one of the settlement systems. Four regressor maps were included in the regression models, a map indicating the travel time to the nearest city (Weiss et al.,

2018), an Euclidean distance map to roads (Meijer, Huijbregts, Schotten, & Schipper, 2018), and an elevation and a slope map (Rabus, Eineder, Roth, & Bamler, 2003). The AUC values for all settlement systems were high, ranging from 0.89 for villages to 0.97 for densely developed urban area, indicating that the allocation of these land systems was explained really well by these explanatory variables (Table S4).

In this model application, settlement system change is driven by a demand for population growth, associated with the service of providing residency to inhabitants. Population growth scenarios are taken from the medium population growth scenario of the World Population Prospects 2019 for each country (United Nations, 2019b). An increase in population can be accommodated by expansion and intensification. Intensification is operationalized by settlement transitions along the rural-urban gradient and towards densely developed urban systems. Expansion, on the other hand, is represented by the conversion of natural and agricultural systems into settlement systems. The population included in each settlement system is determined for each country separately, based on the gridded population data from the GHSL (Schiavina et al., 2019). This approach implicitly assumes that all pixels of a settlement system within a country provide housing to the same number of residents. Demand for population and population residing in settlement pixels are presented in Tables S5 and S9.

As a population becomes wealthier, household size decreases, increasing the total demand for residential area even where population growth reverses (Bradbury, Peterson, & Liu, 2014). Data from the UN Household Size and Composition 2019 database indicated a sharp decline in household sizes over time throughout the study region (United Nations, 2019a). We expect this trend to continue and included a 10% decrease in population density in all settlements systems in 2040, and interpolated for the years in between. Projections for Thailand and Vietnam show a declining population near the end of the simulation period. However, this population decline is smaller than the decrease in household size, and therefore there is no need for land systems to convert backward along the rural-urban gradient (i.e. towards villages).

In the urban expansion scenario, development of agricultural land into a residential area may take place, because of policy decisions, increased mobility or lower land prices be more profitable to developers then further development of existing urban area. On the other hand, policies aimed at compact city development may inhibit expansion of residential land systems through spatial planning. A conversion resistance representing the relative ease of land system conversion was adjusted to represent these different scenarios. By reducing the conversion resistance of agricultural and natural systems, settlement expansion is favored over intensification. Conversely, intensification was simulated by increasing the conversion resistance of agricultural and natural land while reducing the resistance within settlement classes. It should be noted that the difference between both scenarios is relative: both projections include urban expansion as well as urban intensification, but they differ in the preference for each of these developments.

We allocate the demand for national population growth for each country separately because this ensures consistency with the national-scale projections and thus avoids for example demand for population growth in Cambodia being allocated in Thailand. The model was run two times for each country separately, once for the intensification scenario and once for the expansion scenario to create two settlement change projections. Conversion resistance values were parameterized based on visual comparison of resulting land system maps with satellite imagery of the twenty-year period between 1995 and 2015 in Google Earth. The model was calibrated so that the magnitude of observed expansion is greater than projected in the intensification scenario and smaller than in the expansion scenario. This process required several model runs after which conversion resistance values were adjusted based on an expert-based evaluation of the simulated urban development. Due to national differences in local suitability, and to yield comparable development simulations, each country required a separate parameter calibration. Since the scenarios represent reasonably contrasting trajectories, rather than an accurate representation of reality, we did not conduct a formal validation of the simulated urban development. A detailed model description and complete overview of all model parameters is provided in the supplementary material.

2.3. Flood risk assessment

We assess flood risk as a function of hazard, exposure, and vulnerability (Koks, Jongman, Husby, & Botzen, 2015). Hazard is operationalized by flood maps with return periods ranging from 10 to 500 years, exposure is operationalized by the economic value of different settlement systems, and vulnerability was operationalized by a depth-damage function for residential structures. The flood risk assessment broadly consisted of three steps. First, the built environment of each settlement system type was characterized based on building material, which is highly indicative of the economic value of different settlements (Englhardt et al., 2019). Buildings were categorized in four damage classes based on their construction material: informal/slum structures, wooden structures, masonry structures, and concrete structures. Second, devaluated construction cost for each building type was calculated based on the GDP per person in the respective countries. Third, a depth-damage curve was assigned to each land system and used to calculate flood damage. Using inundation maps of 10- to 500-year return periods, flood risk was estimated in terms of expected annual damage for each country and for each land change projection.

We determined the building material within each class based on visual inspection of settlement systems as revealed in Google Earth imagery. Random samples of settlement grid cells were visually inspected to determine whether the settlement classification procedure captured differences in built environments. For each country, 40 images were evaluated per settlement type, distributed over ten randomly selected grid cells using the random point generator in ArcGIS Pro. For each image, we recorded the fraction of buildings from each damage class. A more detailed description and example of this procedure is presented in Figs. S1-2. Estimates of building composition are shown in Fig. 2. The sample size applied here is potentially insufficient to capture the full heterogeneity of the built environment in each country and introduces uncertainty in the representation of built-up land. Representation of built-up land can be greatly improved by information on building materials commonly used in the area. However, since datasets on building material are currently unavailable, we assume the results of our visual assessment to be indicative for the built environment of countries assessed in the study area. The use of building material in each settlement class remained static during the simulation period. We acknowledge that as populations become wealthier, the use of more expensive materials, such as masonry is expected to increase. Static representation of building material likely underestimates actual future damages A conversion factor of 0.4 based on Huizinga et al. (2017) was used to convert built-up area to building footprint. The average built-up density of each settlement system of a country was extracted from the GHSL Built-up dataset.

The maximum potential damage to all buildings in a settlement type cell was calculated based on construction cost with methods adapted from Englhardt et al. (2019) and Huizinga et al. (2017). Where Englhardt et al. (2019) developed separate depth-damage curves for each building class, here a single curve is applied with different exposure values:

$$C = a^{*}GDP_{PC}{}^{*}b \quad (1)$$

Where C is construction cost per square meter in Euro's, GDP_{PC} is the gross domestic product per capita, and a and b parameters provided by Huizinga et al. (2017). Values for GDP_{PC} and construction costs are presented in Tables 1 and 2. The adjusted reconstruction cost for building class k is then calculated by:

$$S_k = C^{*}C_{depricated}{}^{*}MaxAdj_k{}^{*}(1 - Undam_k) \quad (2)$$

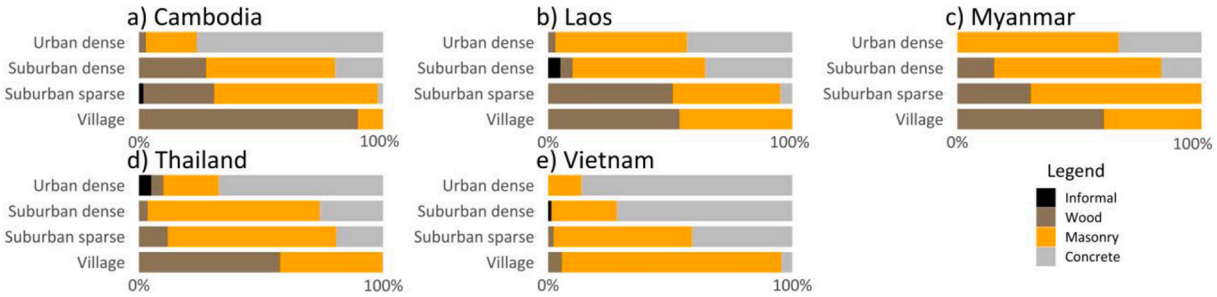

Fig. 2. Distribution of building material found in each settlement class according to our analysis based on Google Earth imagery. The settlement classes urban dense, suburban dense, suburban sparse and village are described in Fig. 1.

Table 1
GDP per capita and construction cost (The World Bank, 2020).

Country	GDP per capita in 2015 [USD 2010]	Construction cost per m^2 [EUR 2010]
Cambodia	1024	348
Laos	1539	407
Myanmar	1335	385
Thailand	5741	675
Vietnam	1667	419

Table 2
Building classes with corresponding adjustment factors (Huizinga et al., 2017).

Building class	Max damage adjustment	Undamaged part	Max inventory
Informal/ slum	0.125	0	0.2
Wood	0.33	0.1	0.5
Masonry	0.8	0.4	0.5
Concrete	1	0.4	0.5

Where S_k is building cost per square meter for a building class k; C is the construction cost per square meter; $C_{depreciated}$ is a conversion factor to calculate the depreciated value of the construction material; $MaxAdj_k$ is the building type specific adjustment factor to account for the use of less expensive building material in building class k; $Undam_k$ is the fraction undamageable of building type k. A depreciated value factor of 0.5 was used for all building classes (Huizinga et al., 2017). Building type specific adjustment factors are listed in Table 3. Next, maximum damage to building content and inventory per square meter was calculated as a function of the building cost:

$$Inv_k = S_k * MaxInv_k \quad (3)$$

Inv_k is the maximum potential damage to building inventory of class k as a function of building cost and conversion factor $maxinv$ for building type k. Subsequently, the maximum potential damage for each cell of settlement class j is calculated following Huizinga et al. (2017):

$$D_j = \sum_{k=1}^{k} (S_k + Inv_k) * N_{j,k} * A_j * CellSize \quad (4)$$

D_j is herein the maximum potential damage for a grid cell of settlement system type j as a sum of the potential damage to all building of types present; $N_{j,k}$ is the fraction of built-up area consisting of building type k in a cell of settlement class j; A is the percentage of a cell covered by building footprint derived from built-up area in pixels of settlement type j; $cellsize$ is the cell size in square meters.

A single depth damage curve for residential buildings in Asia provided by (Huizinga et al., 2017) was applied with inundation maps of 10-, 20-, 50-, 100- and 500-year return periods provided by Dottori et al. (2016). The modeled flood maps represent probabilistic inundation maps for the entirety of the region under current climate conditions.

In applying residential building damage calculations to all buildings in a settlement system cell, we base our calculations of potential damages as if all buildings were residential. Since other building types, for example commercial buildings, can constitute higher damages more often than lower damages, we expect that estimated damage results are slightly underestimated. The only way to include specifically different building types in our assessment is by using generic fixed proportions. As in this study we are interested in the changes between the scenarios, such a fixed proportion would not meaningfully affect our findings.

Table 3
Expected annual damage in settlements (in million 2010 EUR).

Country	Initial 2015	Expansion 2040	Net increase	Intensification 2040	Net increase
Cambodia	237	601	153%	624	162%
Laos	249	727	191%	776	211%
Myanmar	700	1209	73%	1126	61%
Thailand	9229	10,730	16%	9926	8%
Vietnam	9677	14,707	52%	11,716	21%

2.4. Comparisons of different representations of urban land

To assess the added value of including four different settlement systems we compared the expected annual damage of our projected land system changes with the flood risk for a situation with only one homogenous class of urban land. The summed value of all settlement systems in the initial map of each country was divided by the total number of settlement pixels to calculate the average settlement pixel exposure values. This value was applied to all settlement systems in each country and compared with the results of our, more detailed, settlement change projections. To put the difference between our results and this simple model in perspective, we also add a confidence interval to our results. For this confidence interval we follow Huizinga et al. (2017), who report a 90% confidence interval of maximum damage values between 28% lower and 53% higher than calculated maximum damage values.

3. Results

3.1. Land system change projections until 2040

Land system change in all countries until 2040 include a combination of expansion and intensification of urban areas, but with different distributions for the different scenarios (Fig. 3). Overall, these images show, as expected, that intensification leads to a larger increase in the more densely populated land systems, while the expansion scenarios shows a larger increase in the more sparsely populated land systems (Fig. 4). However, the exact manifestations of land system changes differ between countries, and depend on the amount of population growth as well as the land system response to the associated demand for housing.

Total area characterized by settlement systems in **Cambodia** increased with 325% in the settlement expansion and 91% in the

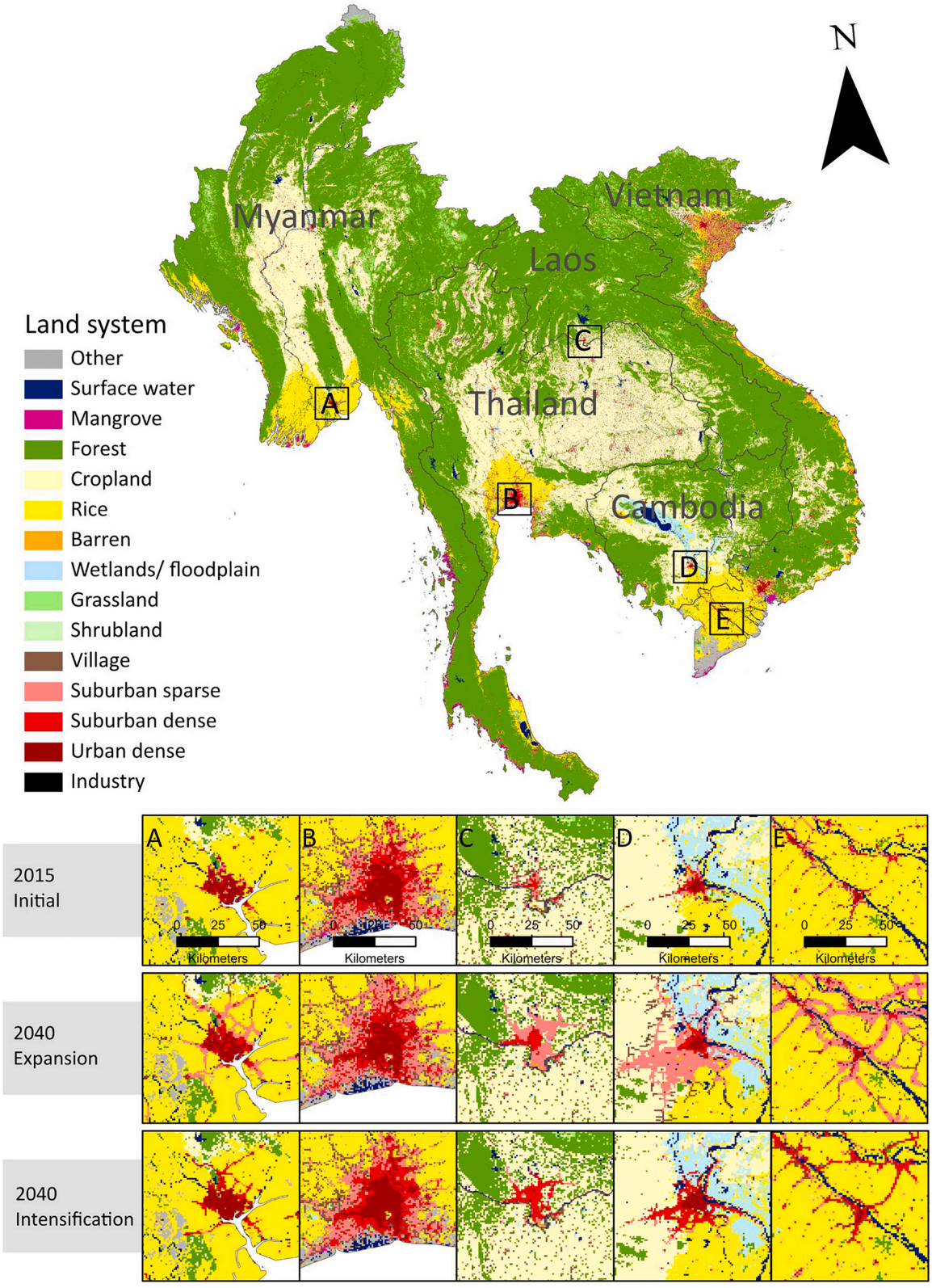

Fig. 3. Land system change in countries of Southeast Asia projected from 2015 to 2040. Shown are snapshots from a. Yangon, b. Bankok, c. Vientiane, d. Phnom Penh, and e. Can Tho.

intensification scenario. Most settlement change occurred in the vicinity of Battambang, Siem Raep, and the capital Phnom Penh. Built-up area increased by 155% and 101% in a settlement expansion and intensification scenario, respectively. The difference between both scenarios is mainly due to the large increase in *Sparse suburban systems* in the expansion scenarios (Fig. 4a), which thus requires a large extent to accommodate the growing population. In the intensification scenario, population increase was predominantly accommodated by converting *Village systems* and Suburban sparse systems into *Suburban dense systems*, and to a lesser extent into *Urban dense*, representing further

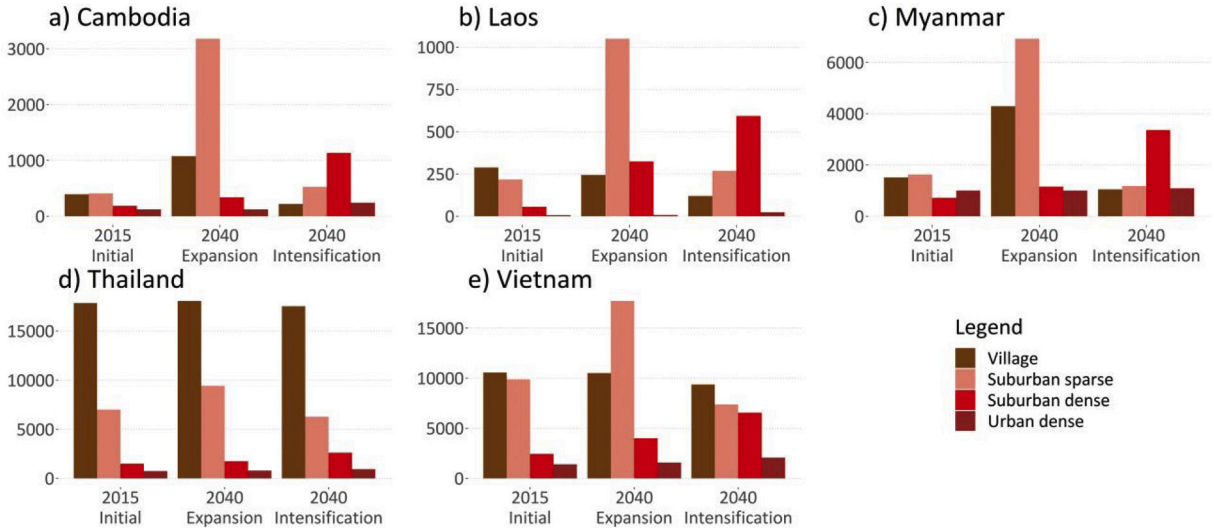

Fig. 4. Area occupied by each settlement system at the beginning and end of the simulation (in km^2).

intensification of existing settlement systems.

In **Laos**, the total settlement area increased by 187% in the settlement expansion and 77% in the settlement intensification scenario. Settlement change mostly occurred near Vientiane, Luang Prabang, and Pakse. Built-up area increased by 156% in the expansion and 128% in the intensification scenario. The increase of built-up land was greater than the extent of settlement expansion in the intensification scenario, indicating further densification of already urbanized land. Note that in 2015 as well as in both scenario outcomes there are only very few pixels characterized as Urban dense, and that intensification mainly leads to an increase in *Suburban dense systems* (Fig. 4b).

Settlement systems in **Myanmar** are rather evenly distributed in the year 2015 (Fig. 4c). The area identified as settlement systems further increased by 175% in the settlement expansion and 37% in the settlement intensification scenario. Remarkably, Myanmar is the only country in which a large increase in *villages* is expected, in the expansion scenario, as other countries mostly see an increase in suburban sparse systems only. Intensification is predominantly manifested in an increase in *Suburban dense* systems. Built-up area increased by 73 and 38%, respectively.

Relatively few settlement changes were simulated in both scenarios in **Thailand**, because population is expected to increase only marginally between 2015 and 2040, and even decrease in the latter years of the simulation period. As a result, settlement area increased by only 11% in the expansion and 1% in the intensification scenario. The corresponding increase in built-up area was 11 and 6%, respectively. The increase in built-up area was greater than the increase in settlement area in both the expansion and intensification scenario, indicating that even the expansion scenario is mainly characterized by urban intensification, but less so than the intensification period (Fig. 4d). Settlement area increased less than the population in the intensification scenario, indicating a general increase of population density.

Total area of settlement systems in **Vietnam** increased 39% in the expansion and 4% in the intensification scenario, while the total amount of built-up land increased by 36 and 18%, respectively. The increase in settlement area was smaller than the increase in population in the intensification scenario, indicating increasing population densities and thus overall urban intensification. Most settlement expansion occurred in the Mekong and Red River deltas. Settlement systems expanded outward of existing cores along access roads. Densely developed urban systems emerged mostly near existing urban cores, although some land transitions occurred along the coast.

3.2. Flood risk in 2040

Potential flood damages increased in all five countries under both development scenarios (Table 3). This increase is a direct result of the urban development in both scenarios as both simulate a further development of new settlement systems as well as urban intensification along the rural-urban gradient. However, the manifestation of settlement system changes differs between scenarios, and so do local characteristics affecting inundation depth (Fig. 5). As a consequence, Flood risk increases more in the intensification scenario in Laos and Cambodia, while it increases more in the urban expansion scenario in Myanmar, Thailand, and Vietnam. We attribute these differences in optimal urban development pathways to the presence of large cities in the floodplains of the Chao Praia-, Irrawaddy- and Mekong River deltas. Contrary to Cambodia and Laos, urban development based on local suitability rarely occurs out of harm's way in these regions. Flood risk curves illustrating flood damage for the different return periods are provided in Fig. S3, here we report on the overall risk in terms of expected annual damage.

In **Cambodia**, flood risk increased most in the settlement intensification scenario. Most flood damages occurred mostly in the city of Phnom Penh, located on the banks of the Tonle Sap and Mekong River. Expected annual flood damage increased by 153% in the settlement expansion and 162% in the intensification scenario. By comparison, settlement systems increased by 325% and 91% in both scenarios. Hence in the intensification scenario, most urban development takes place in areas that are prone to flood risk. Conversely, in the expansion scenario, most settlement change is allocated in areas that are less prone to flooding.

Urban intensification in **Laos** resulted in a greater increase in flood risk than settlement expansion. Expected annual flood damage almost tripled for both scenarios with a 191% increase in the settlement expansion and 211% increase in the settlement intensification scenario. Vientiane was most affected by increased flood risk due to its location next to the Mekong River.

Flood risk in **Myanmar** increased most in the expansion scenario. Expected annual flood damage increased with 73% in the expansion and 61% in the settlement intensification scenario. Most affected by increased flood risk were Mandalay and Yangon, located on the banks and in the delta of the Irrawaddy River.

In **Thailand**, as well as in Vietnam, flood risk is an order of magnitude higher than in the other three countries. At the same time, due to the relatively small amount of urban development, flood risk increases only little in both scenarios. Flood risk increased most in the settlement expansion scenario. Expected annual flood damage increased by 16% in the expansion and 8% in the settlement intensification scenario, most of

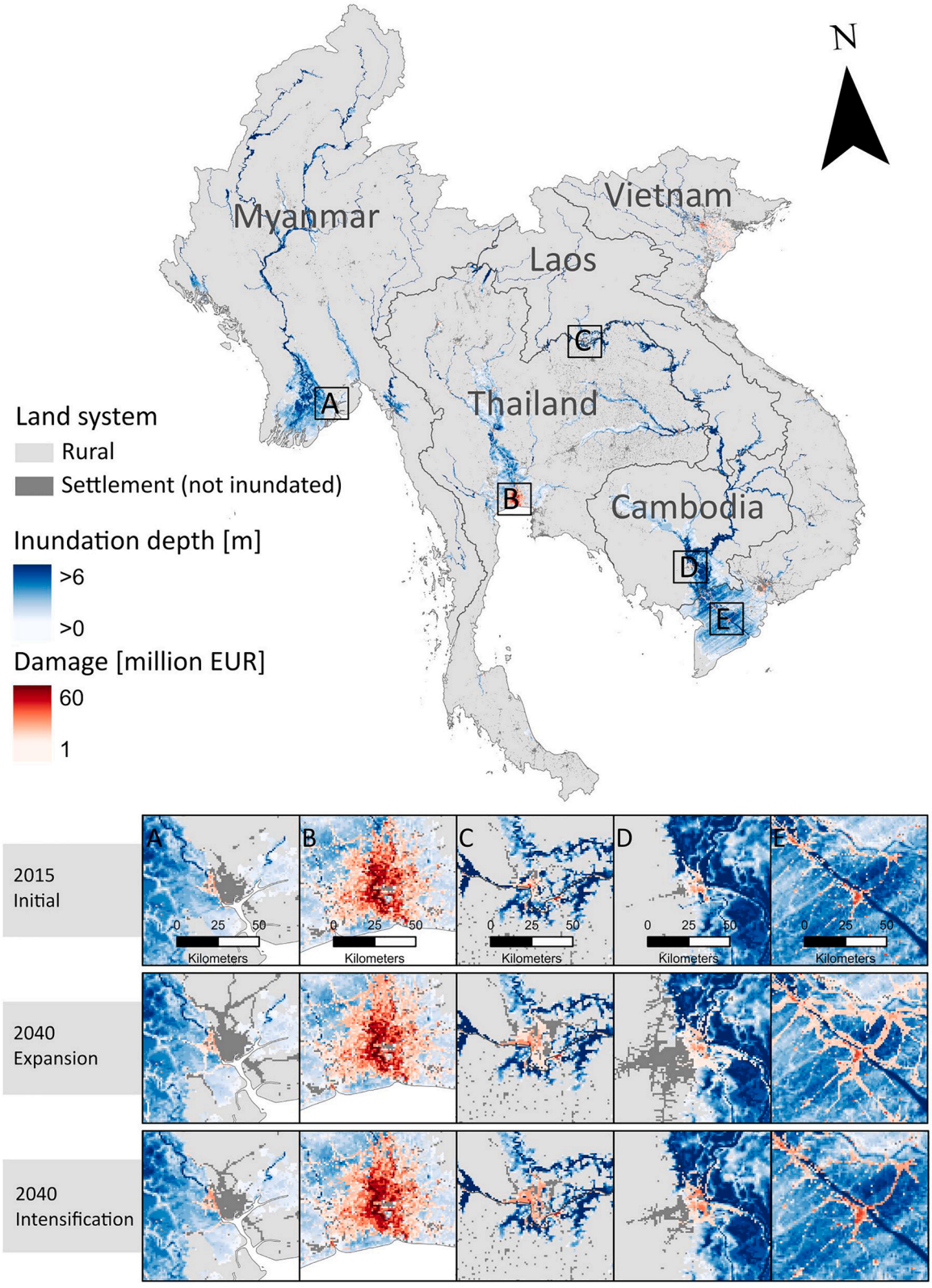

Fig. 5. Estimated flood damage maps for a 10-year return period for the entire study area as well as for a. Rangoon, b. Bangkok, c. Vientiane, d. Phnom Penh, and e. Can Tho. The inundation map shown in this figure is based on Dottori et al. (2016).

which is in and around Bangkok, located in the Chao Praia delta.

Vietnam includes the deltas of both the Red River and the Mekong River and these areas are relatively densely inhabited, thus leading to the high flood risk as compared to Cambodia, Laos and Myanmar already in 2015. Until 2040, flood risk increases most in the settlement expansion scenario in flooding considering all return periods, again mostly affecting both river deltas. However, contrary to Thailand, which also has a high flood risk in 2015, the estimated damages in flooding increase considerably in Vietnam, with a 52% increase in the expansion and a 21% increase in the intensification scenario.

3.3. Comparisons of different representations of urban land

A comparison of model results with a more simplistic representation of one type of building composition shows that the expected annual damage based on the simple land system representation is lower in all countries and for all years, except for the expansion scenario in Myanmar (Table 4). The simplified representation of built-up land fails to capture the high asset value of densely developed urban area prone to flooding. Aggregating all settlement land in a single class demonstrated the need for differentiating exposed asset values when assessing optimal urban development strategies. More importantly, a closer look at the simulated changes reveals important differences. As using a single settlement class only increases flood damage when the urban area increases, our analysis reveals that in these calculations the expansion scenario will always yield the largest increase in flood risk, whilst our analysis shows the opposite for Cambodia and Laos (where the intensification scenarios gives the largest increase in flood risk).

4. Discussion

4.1. Urban development and exposure to river flooding in Southeast Asia

Expected annual damage as a result of river flooding in Southeast Asia is projected to increase between 8% in Thailand and 211% in Laos as a result of urban development until 2040. This large increase is consistent with findings by Jongman et al. (2012) and Winsemius et al. (2016). The difference between these two extremes can be explained mostly by the expected population growth in combination with the initial situation. Thailand is already fairly urbanized and expects only a small population growth until 2040. As a result, our model projects only little urban development. Conversely, population in Laos is expected to grow much faster, while there was only little urban land in the 2015. Here the relative increase in urban land is large.

The impact of different urban development pathways on expected annual damages varied among countries. Furthermore, optimal development pathways resulted in lowest flood damage for all return periods assessed in this study (Fig. S3). In Cambodia and Laos, settlement intensification resulted in higher expected annual flood damages. In Myanmar, Thailand, and Vietnam we found urban expansion to result in higher expected annual flood damage. Only few other studies made such comparative assessment between different urban development scenarios, as land system models are typically unable to make such differentiation (Wang et al., 2019). One example is Mustafa et al. (2018), who found that in Belgium urban intensification resulted in higher flood damages compared to urban expansion in 2100, which is similar to our finding for Laos and Cambodia. Other studies have pointed at the large urban development in flood-prone areas in Southeast Asia but did not compare different urban development pathways (e.g. Storch and Downes (2011)).

Table 4
Comparison of expected annual damage (in million 2010 EUR) obtained from our analysis with comparable results in which only one class of urban land was presented within each country.

Country	Scenario	Expected annual flood damage (+90% confidence interval)	Expected annual flood damage with a single settlement class
Cambodia	Initial (2015)	237 (171–363)	132
	Expansion 2040	601 (433–920)	523
	Intensification 2040	624 (449–954)	275
Laos	Initial (2015)	249 (178–382)	206
	Expansion 2040	727 (523–1112)	452
	Intensification 2040	776 (559–1187)	324
Myanmar	Initial (2015)	700 (504–1071)	639
	Expansion 2040	1209 (870–1849)	1225
	Intensification 2040	1126 (810–1722)	805
Thailand	Initial (2015)	9229 (6645 - 14,120)	4524
	Expansion 2040	10,730 (7725 - 16,417)	5040
	Intensification 2040	9926 (7147 - 15,187)	4721
Vietnam	Initial (2015)	9677 (6967 - 14,806)	6802
	Expansion 2040	14,707 (10,589 - 22,502)	10,378
	Intensification 2040	11,716 (8435 - 17,925)	8330

Underlined values show the scenario for which the increase in expected annual damage is largest, per country.

Comparisons of expected annual damage values to recorded flood damage prove difficult, as recorded damages are often only available for high impact events and yearly damage fluctuates. For example, recorded flood damages in Thailand in the period between 1980 and 2018 amount up to 51 billion USD, of which 42 billion USD originated from flooding in the year 2011 alone (Munich, 2020). Countries may not encounter significant flooding for years, and a single destructive event may greatly increase the expected annual damages. The occurrence of a flood may furthermore influence urban development in affected areas. The experience of flooding heightens both the individual and institutional perception of risk, prompting governments and people to vacate parts of the floodplain through managed retreat, hereby lowering the exposed asset value (Burningham, Fielding, & Thrush, 2008; Hino, Field, & Mach, 2017). However, this learning effect often decays over time, and with construction of levees disaster-struck areas may again experience rapid population growth within decades after the flood event (Collenteur, De Moel, Jongman, & Di Baldassarre, 2015). Considering the projected increase in both river flood frequency- and severity due to climate change, the impact of river flooding on urban development requires attention in future research (Hirabayashi et al., 2013).

Sea level rise in combination with land subsidence poses a more permanent threat on urban development in coastal regions of the study area (Erban, Gorelick, & Zebker, 2014). Increased severity and frequency of storm surges, coastal erosion, and permanent inundation may push urban development further inland (Davis, Bhattachan, D'Odorico, & Suweis, 2018; Hauer, 2017). Migration induced by sea level rise not only impacts settlement development in low-lying coastal zones, it increases the demand for residential development in migrant destinations as well (McLeman, 2018). To assess the impact of sea level rise on future urban development, more research on the extent of migration brought about by sea level rise is recommended.

Projection of urban development in a settlement expansion and settlement intensification scenario yielded two rather contrasting outcomes. As we do not know how urban land develops in the future, addressing the diversity of possible urban environments in large scale studies related to human-environmental interactions is paramount to account for uncertainties in urban development. Since the classification of urban land widely differs among studies (Liu, He, Zhou, & Wu, 2014), comparisons to past settlement change provides a challenge. Here we compared observed changes in built-up area in the Global Human Settlement layer with projected built-up change (Table 5). The projected average annual growth rate of built-up area in Cambodia and Laos is greater than the observed growth rate in the period between 2000 and 2015 in both scenarios. Since only settlement systems respond to an increased demand for population, these less urbanized countries experienced a relatively greater increase in settlement area compared to countries that were already more urbanized. In Myanmar and Vietnam, averaged annual growth rates in the period between 2000 and 2015 lies in between the growth rate of both projections. Thailand experienced a greater annual increase in built-up area in the period between 2000 and 2015 than in the both settlement change projections. This could be a result of the expected population growth rate, which is much lower until 2040 than in the period 2000–2015. In addition, recent decades are characterized by rapid urban expansion due to rural-urban migration in combination with economic development, leading to the rapid growth of

Table 5
Observed annual growth rate (AGR) of built-up area (km^2) in the Global Human Settlement Layer versus the projected AGR. Slight differences for the year 2015 exist because the total built-up area in the modeled change was derived from averaged built-up area in land systems.

Country	GHSL			Initial	Expansion		Intensification	
	2000	2015	AGR	2015	2040	AGR	2040	AGR
Cambodia	247	324	1.83%	322	819	3.81%	646	2.83%
Laos	110	165	2.71%	162	397	3.64%	370	3.36%
Myanmar	1084	1366	1.55%	1350	2338	2.22%	1856	1.28%
Thailand	5240	6639	1.59%	6609	7306	0.40%	7020	0.24%
Vietnam	4822	5712	1.14%	5711	7770	1.24%	6760	0.68%

especially Bangkok. While the economic development is expected to continue, much of the urban infrastructure for this development is now already available.

4.2. Sustainable urban planning

Urban flood risk management, incorporating all aspects of risk, is replacing more traditional approaches aimed primarily at controlling flood hazard (Ran & Nedovic-Budic, 2016). Here we enhanced the representation of exposure by a more elaborate characterization of human settlement. We showed that the accumulation of asset value in already urbanized environments in an intensification scenario does not always result in higher flood damage when compared to expansion. On the other hand, urban expansion does not always result in urban development out of harm's way. Urban planners in Cambodia and Laos need to consider increased flood risk when policy opts for compact development or urban containment strategies opposed to unregulated sprawl, as this development pathway will exacerbate future damages by increasing the exposed asset value. Burby, Nelson, Parker, and Handmer (2001) identified this process as a side-effect of 'smart growth', urging planners to adjust building techniques and to invest in flood protection infrastructure. In contrast, city planners in Thailand, Myanmar, and Vietnam are presented with an incentive to opt for compact city development, as urban expansion will result in higher damages when compared to compact development. Settlement expansion in these regions occurs mainly in large river deltas, meaning that settlement expansion out of harm's way from existing urban cores is not an option. Governments could opt to channel urban development further inland and away from river deltas. However, considering the cost of building the infrastructure to support these new cities zonal planning and infill development may prove to be the preferable strategy to mitigate the effects of urban development to flooding.

However, as institutional changes in urban planning are slow and considering the short time-period addressed in this study, site-specific adaptations may be more feasible. Adaptations discussed by Lasage et al. (2014) include wet-proofing and dry-proofing of buildings. Dry-proofing buildings is aimed at preventing water from entering the building by reinforcing both structure and sewage systems. This method is especially effective for water levels less than 1 m, as higher water pressure results in structural failure (de Moel, van Vliet, & Aerts, 2014). Dry-proofing buildings may significantly reduce flood damages in deltas with relatively low inundation levels in for example Bangkok and Ho Chi Minh city by decreasing the vulnerability of building types. Wet-proofing entails building adaptations that decrease damage in case water has entered the building. Adaptations are relatively easy to implement, by for example raising electricity sockets and valuable appliances to higher floors. This method is effective for water levels up to 3 m, making it more suitable for buildings exposed to higher inundation levels in for example Phnom Penh and Vientiane (Lasage et al., 2014).

5. Conclusion

In this study we analyzed future flood risk under two different urban development scenarios using a novel approach to simulate urban development. Projecting urban development in an urban expansion and intensification scenario resulted in two contrasting land use maps. Flood damage estimations showed flood risk to increase in all countries of the study area. Laos was most affected, with expected annual flood damage increasing by 211% in the urban intensification scenario. Optimal development pathways were shown to be context dependent. In Cambodia and Laos flood risk increased least in an urban expansion scenario. In Myanmar, Thailand and Vietnam flood risk increased least in an urban intensification scenario. Differences in expected annual damage between the two urban development scenarios were greatest in Vietnam, with a 52% increase in an expansion versus a 21% increase in an urban intensification scenario. Optimal development pathways hold true for all different return periods. Sustainable urban development policies in Cambodia and Laos could consider that urban containment and compact development strategies exacerbate future flood damage through increased exposure. In Myanmar, Thailand and Vietnam the presence of major river deltas resulted in settlement development occurring mostly on areas prone to flooding. This meant that contradictory to Cambodia and Laos development out of harm's way rarely occurred. Although we enhance the representation of the built environment by moving beyond the representation of urban area in a single class, flood damage estimations could benefit from more detailed information on the building materials commonly found in different regions of the study area. In light of climate change, we recommend further research on the impact of extreme flood events and sea level rise on urban development in the study region. This study revealed the complicating effect of different urban development pathways on flood damage estimations and identified optimal development strategies for mitigating future flood risk in Southeast Asia.

Competing interests

The authors declare no competing interests.

Acknowledgements

JvV was supported by the Netherlands Organization for Scientific Research NWO (Grant No VI.Vidi.198.008).

Appendix A. Supplementary data

Supplementary data to this article can be found online at https://doi.org/10.1016/j.compenvurbsys.2021.101620.

References

van Asselen, S., & Verburg, P. H. (2013). Land cover change or land-use intensification: Simulating land system change with a global-scale land change model. *Global Change Biology, 19*(12), 3648–3667.

Bradbury, M., Peterson, M. N., & Liu, J. (2014). Long-term dynamics of household size and their environmental implications. *Population and Environment, 36*(1), 73–84.

Burby, R. J., Nelson, A. C., Parker, D., & Handmer, J. (2001). Urban containment policy and exposure to natural hazards: Is there a connection? *Journal of Environmental Planning and Management*. https://doi.org/10.1080/09640560125021.

Burningham, K., Fielding, J., & Thrush, D. (2008). 'It'll never happen to me': understanding public awareness of local flood risk. *Disasters, 32*(2), 216–238.s.

Collenteur, R. A., De Moel, H., Jongman, B., & Di Baldassarre, G. (2015). The failed-levee effect: Do societies learn from flood disasters? *Natural Hazards, 76*(1), 373–388.
Corbane, C., Florczyk, A., Pesaresi, M., Politis, P., & Syrris, V. (2018). *GHS built-up grid, derived from Landsat, multitemporal (1975-1990-2000-2014), European Commission, Joint Research Centre (JRC)*. https://doi.org/10.2905/jrc-ghsl-10007.
Davis, K. F., Bhattachan, A., D'Odorico, P., & Suweis, S. (2018). A universal model for predicting human migration under climate change: Examining future sea level rise in Bangladesh. *Environmental Research Letters, 13*(6), Article 064030.
Delso, D. (2013). View of Ho Chi Minh City from Bitexco Financial Tower, Vietnam. https://nl.m.wikipedia.org/wiki/Bestand:Vista_de_Ciudad_Ho_Chi_Minh_desde_Bitexco_Financial_Tower,_Vietnam,_2013-08-14,_DD_06.JPG.
Dottori, F., Salamon, P., Bianchi, A., Alfieri, L., Hirpa, F. A., & Feyen, L. (2016). Development and evaluation of a framework for global flood hazard mapping. *Advances in Water Resources, 94*, 87–102.
Englhardt, J., de Moel, H., Huyck, C. K., de Ruiter, M. C., Aerts, J. C. J. H., & Ward, P. J. (2019). Enhancement of large-scale flood risk assessments using building-material-based vulnerability curves for an object-based approach in urban and rural areas. *Natural Hazards and Earth System Sciences, 19*(8).
Erban, L. E., Gorelick, S. M., & Zebker, H. A. (2014). Groundwater extraction, land subsidence, and sea-level rise in the Mekong Delta, Vietnam. *Environmental Research Letters, 9*(8), Article 084010.
Ewing, R. H., Pendall, R., & Chen, D. D. T. (2002). *Measuring sprawl and its impact. 1*. Washington, DC: Smart Growth America.
Google Earth. (2020a). Krouch Chhmar, Cambodia. 12°16′21.5″N 105°39′07.4″E. https://www.google.nl/intl/nl/earth/.
Google Earth. (2020b). Pakse, Laos. 15°07′00.7″N 105°49′14.6″E. https://www.google.nl/intl/nl/earth/.
Google Earth. (2020c). Bangkok, Thailand. 13°39′11.9″N 100°35′30.2″E. https://www.google.nl/intl/nl/earth/.
Hahs, A. K., & McDonnell, M. J. (2006). Selecting independent measures to quantify Melbourne's urban–rural gradient. *Landscape and Urban Planning, 78*(4), 435–448.
Hauer, M. E. (2017). Migration induced by sea-level rise could reshape the US population landscape. *Nature Climate Change, 7*(5), 321–325.
Hino, M., Field, C. B., & Mach, K. J. (2017). Managed retreat as a response to natural hazard risk. *Nature Climate Change, 7*(5), 364–370.
Hirabayashi, Y., Mahendran, R., Koirala, S., Konoshima, L., Yamazaki, D., Watanabe, S., … Kanae, S. (2013). Global flood risk under climate change. *Nature Climate Change*. https://doi.org/10.1038/nclimate1911.
Huizinga, J., de Moel, H., Szewczyk, W., & others. (2017). *Global flood depth-damage functions: Methodology and the database with guidelines (No. JRC105688)*. Joint Research Centre (Seville site).
Jongman, B., Ward, P. J., & Aerts, J. C. J. H. (2012). Global exposure to river and coastal flooding: Long term trends and changes. *Global Environmental Change, 22*(4), 823–835.
Koks, E. E., Jongman, B., Husby, T. G., & Botzen, W. J. W. (2015). Combining hazard, exposure and social vulnerability to provide lessons for flood risk management. *Environmental Science & Policy, 47*, 42–52.
Kroll, F., Müller, F., Haase, D., & Fohrer, N. (2012). Rural–urban gradient analysis of ecosystem services supply and demand dynamics. *Land Use Policy, 29*(3), 521–535.
Lasage, R., Veldkamp, T. I. E., de Moel, H., Van, T. C., Phi, H. L., Vellinga, P., & Aerts, J. C. J. H. (2014). Assessment of the effectiveness of flood adaptation strategies for HCMC. *Natural Hazards and Earth System Sciences*. https://doi.org/10.5194/nhess-14-1441-2014.
Li, M., van Vliet, J., Ke, X., & Verburg, P. H. (2019). Mapping settlement systems in China and their change trajectories between 1990 and 2010. *Habitat International, 94*, 102069.
Liu, Z., He, C., Zhou, Y., & Wu, J. (2014). How much of the world's land has been urbanized, really? A hierarchical framework for avoiding confusion. *Landscape Ecology*. https://doi.org/10.1007/s10980-014-0034-y.
McDonnell, M. J., & Pickett, S. T. (1990). Ecosystem structure and function along urban-rural gradients: An unexploited opportunity for ecology. *Ecology, 71*(4), 1232–1237.
McLeman, R. (2018). Migration and displacement risks due to mean sea-level rise. *Bulletin of the Atomic Scientists, 74*(3), 148–154.
Meijer, J. R., Huijbregts, M. A. J., Schotten, K. C. G. J., & Schipper, A. M. (2018). Global patterns of current and future road infrastructure. *Environmental Research Letters, 13*(6), 64006.
de Moel, H., Jongman, B., Kreibich, H., Merz, B., Penning-Rowsell, E., & Ward, P. J. (2015). Flood risk assessments at different spatial scales. *Mitigation and Adaptation Strategies for Global Change, 20*(6), 865–890.
de Moel, H., van Vliet, M., & Aerts, J. C. J. H. (2014). Evaluating the effect of flood damage-reducing measures: A case study of the unembanked area of Rotterdam, the Netherlands. *Regional Environmental Change*. https://doi.org/10.1007/s10113-013-0420-z.
Munich, R. E. (2020). NatCatSERVICE. https://natcatservice.munichre.com/.
Mustafa, A., Bruwier, M., Archambeau, P., Erpicum, S., Pirotton, M., Dewals, B., & Teller, J. (2018). Effects of spatial planning on future flood risks in urban environments. *Journal of Environmental Management*. https://doi.org/10.1016/j.jenvman.2018.07.090.
Patterson, M. S., Tenneson, K., Cherrington, E. A., Ellenburg, W. L., Markert, K. N., Ate, P., … others. (2018). *Documenting and distributing a regional land cover monitoring system using free data and cloud-based computing infrastructure in the lower Mekong countries in Southeast Asia* (AGU Fall Meeting Abstracts).
Rabus, B., Eineder, M., Roth, A., & Bamler, R. (2003). The shuttle radar topography mission—A new class of digital elevation models acquired by spaceborne radar. *ISPRS Journal of Photogrammetry and Remote Sensing, 57*(4), 241–262.
Ran, J., & Nedovic-Budic, Z. (2016). Integrating spatial planning and flood risk management: A new conceptual framework for the spatially integrated policy infrastructure. *Computers, Environment and Urban Systems*. https://doi.org/10.1016/j.compenvurbsys.2016.01.008.
Schiavina, M., Freire, S., & MacManus, K. (2019). GHS population grid multitemporal (1975, 1990, 2000, 2015) European Commission, Joint Research Centre (JRC). http://data.europa.eu/89h/0c6b9751-a71f-4062-830b-43c9f432370f.
Storch, H., & Downes, N. K. (2011). A scenario-based approach to assess Ho Chi Minh City's urban development strategies against the impact of climate change. *Cities.*. https://doi.org/10.1016/j.cities.2011.07.002.
Storch, H., Eckert, R., & Pfaffenbichler, P. (2008). *The compactness of urban areas in Vietnam. Sustainable urban development and local mobility nodes*. REAL CORP.
The World Bank. (2011). The world bank supports Thailand's post-floods recovery effort. https://www.worldbank.org/en/news/feature/2011/12/13/world-bank-supports-thailands-post-floods-recovery-effort.
The World Bank. (2020). World Bank national accounts data*, and OECD national accounts data files*. https://data.worldbank.org/indicator/NY.GDP.PCAP.CD (Accessed 30 March 2020).
United Nations. (2019a). Database on household size and composition 2019. https://population.un.org/Household/ (Accessed 30 March 2020).
United Nations. (2019b). World population prospects 2019. *Online Edition. Rev. 1* https://population.un.org/wpp/Download/Standard/Population/ (Accessed 30 March 2020).
Varis, O., Kummu, M., & Salmivaara, A. (2012). Ten major rivers in monsoon Asia-Pacific: An assessment of vulnerability. *Applied Geography*. https://doi.org/10.1016/j.apgeog.2011.05.003.
Vinke, K., Martin, M. A., Adams, S., Baarsch, F., Bondeau, A., Coumou, D., … Svirejeva-Hopkins, A. (2017). Climatic risks and impacts in South Asia: Extremes of water scarcity and excess. *Regional Environmental Change*. https://doi.org/10.1007/s10113-015-0924-9.
van Vliet, J., Verburg, P. H., Grădinaru, S. R., & Hersperger, A. M. (2019). Beyond the urban-rural dichotomy: Towards a more nuanced analysis of changes in built-up land. *Computers, Environment and Urban Systems, 74*, 41–49.
Wandl, D. I. A., Nadin, V., Zonneveld, W., & Rooij, R. (2014). Beyond urban–rural classifications: Characterising and mapping territories-in-between across Europe. *Landscape and Urban Planning, 130*, 50–63.
Wang, Y., van Vliet, J., Pu, L., & Verburg, P. H. (2019). Modeling different urban change trajectories and their trade-offs with food production in Jiangsu Province, China. *Computers, Environment and Urban Systems*. https://doi.org/10.1016/j.compenvurbsys.2019.101355.
Ward, P. J., Jongman, B., Weiland, F. S., Bouwman, A., van Beek, R., Bierkens, M. F. P., … Winsemius, H. C. (2013). Assessing flood risk at the global scale: Model setup, results, and sensitivity. *Environmental Research Letters, 8*(4), 44019.
Webster, D., Cai, J., & Muller, L. (2014). The new face of peri-urbanization in East Asia: Modern production zones, middle-class lifesytles, and rising expectations. *Journal of Urban Affairs, 36*(sup1), 315–333.
Weiss, D. J., Nelson, A., Gibson, H. S., Temperley, W., Peedell, S., Lieber, A., … others. (2018). A global map of travel time to cities to assess inequalities in accessibility in 2015. *Nature, 553*(7688), 333–336.
Winsemius, H. C., Aerts, J. C. J. H., van Beek, L. P. H., Bierkens, M. F. P., Bouwman, A., Jongman, B., … others. (2016). Global drivers of future river flood risk. *Nature Climate Change, 6*(4), 381–385.
Winsemius, H. C., van Beek, L. P. H., Jongman, B., Ward, P. J., & Bouwman, A. (2013). A framework for global river flood risk assessments. *Hydrology and Earth System Sciences*. https://doi.org/10.5194/hess-17-1871-2013.